Available online at www.sciencedirect.com
ScienceDirect
Biomaterials 29 (2008) 1233–1241
Biomaterials
www.elsevier.com/locate/biomaterials

Pharmacokinetics, biodistribution, efficacy and safety of *N*-octyl-*O*-sulfate chitosan micelles loaded with paclitaxel

Can Zhang [a], Guowei Qu [a], Yingji Sun [b], Xiaoli Wu [a], Zhong Yao [a], Qinglong Guo [a], Qilong Ding [a], Shengtao Yuan [c], Zilong Shen [b], Qineng Ping [a,*], Huiping Zhou [d]

[a] *College of Pharmacy, China Pharmaceutical University, Nanjing 210009, PR China*
[b] *College of Life Science and Technology, China Pharmaceutical University, Nanjing 210009, PR China*
[c] *The Drug National Screening Center, China Pharmaceutical University, Nanjing 210009, PR China*
[d] *Department of Microbiology and Immunology, School of Medicine, Virginia Commonwealth University, Richmond, VA 23298, USA*

Received 23 August 2007; accepted 12 November 2007
Available online 18 December 2007

Abstract

Paclitaxel (Taxol®, PTX) is a promising anti-cancer drug and has been successfully used to treat a wide variety of cancers. Unfortunately, serious clinical side effects are associated with it, which are caused by PTX itself and non-aqueous vehicle containing Cremophor EL. Development of new formulation of PTX with better efficacy and fewer side effects is extremely urgent. In the present study, a *N*-octyl-*O*-sulfate chitosan (NOSC) micelle was developed and used as the delivery system for PTX. The pharmacokinetics, biodistribution, efficacy and safety of PTX-loaded NOSC micelles (PTX-M) were evaluated. The results showed that NOSC micelles had high drug loading capacity (69.9%) and entrapment efficiency (97.26%). The plasma AUC of PTX-M was 3.6-fold lower than that of Taxol®; but the V_d and CL of PTX-M were increased by 5.7 and 3.5-fold, respectively. Biodistribution study indicated that most of the PTX were distributed in liver, kidney, spleen, and lung and the longest retention effect was observed in the lung. Drug safety assessment studies including acute toxicity, hemolysis test, intravenous stimulation and injection anaphylaxis revealed that the PTX-M was safe for intravenous injection. Furthermore, the comparable antitumor efficacy of PTX-M and Taxol® was observed at the same dose of 10 mg/kg in in vivo antitumor mice models inoculated with sarcoma180, enrich solid carcinoma (EC), hepatoma solidity (Heps), Lewis lung cancer cells and A-549 human lung cancer cells. These results clearly showed that PTX-M had the similar antitumor efficacy as Taxol®, but significantly reduced the toxicity and improved the bioavailability of PTX.

Keywords: Chitosan derivative micelle; Paclitaxel; Pharmacokinetics; Biodistribution; Antitumor efficacy; Safety study

1. Introduction

Paclitaxel (PTX), one of the most exciting anti-cancer agents currently available [1], has been demonstrated significantly active in clinical trials against a wide variety of tumors, including refractory ovarian cancer, metastatic breast cancer, non-small cell lung cancer, AIDS-related Kaposi's sarcoma, head and neck malignancies and other cancers [2,3]. Due to its poor water solubility (<1 μg/mL), PTX is currently formulated in a 50/50 (V/V) mixture of Cremophor EL/absolute ethanol as Taxol®. However, the toxic side effects associated with Taxol, such as hypersensitivity, nephrotoxicity and neurotoxicity [4], lay major obstacles for successful chemotherapy with PTX. A significant amount of effort has been directed to the development of alternative delivery systems for PTX, which has good aqueous solubility and fewer side effects. Several different approaches have been used for development of desired formulations of PTX, such as nanospheres [5], liposomes [6], cyclodextrin complexes [7], emulsions [8], water-soluble prodrugs [9], and polymeric micelles [10,11]. However, the

* Corresponding author. Tel.: +86 25 8327 1098; fax: +86 25 8330 1606.
E-mail address: pingqn@cpu.edu.cn (Q. Ping).

0142-9612/$ - see front matter © 2007 Elsevier Ltd. All rights reserved.
doi:10.1016/j.biomaterials.2007.11.029

ideal dosage form which could bypass all the present limitations and retain the therapeutic efficacy is still lacking.

Recently, an increasing amount of attention has been paid to use polymeric micelles as novel colloidal delivery systems that can fulfill the requirements of an ideal and versatile drug carrier [12]. Polymeric micelles are formed by self-assembly in an aqueous environment and possess a core-shell structure. The hydrophobic core acts as a micro-reservoir for the encapsulation of hydrophobic drugs, proteins or DNA, and the hydrophilic shell interfaces the biological media. Polymeric micelles have been proven as efficient drug delivery systems for intravenous administration because of their attractive characteristics such as smaller size (<100 nm), a propensity to evade scavenging by the mononuclear phagocyte system (MPS) [13], low toxicity, and faster clearance rate from the body.

A number of natural or synthetic polymers have been used to form polymeric micelles. Among them, chitosan, a polysaccharide derived from chitin by complete or incomplete alkaline deacetylation, is the most attractive candidate due to its biochemical activity, biocompatibility, biodegradability and low toxicity [14], and has been widely used in pharmaceutical and nutritional formulations. Chitosan-based nanoparticles [15], microspheres [16], hydrogels [17], films [18], fibers [19] and tablets [20] have been developed, and their biological activities have also been extensively investigated [21]. The unique structure of chitosan, consisting of 2-amino-2-deoxy-β-D-glucopyranose and 2-amino-2-acetamido-β-D-glucopyranose linked with β-(1 → 4) bonds, makes it soluble in aqueous solutions of various acids. However, chitosan has no amphiphilicity and cannot form micelle. During last decade, chitosan-based micelle system has been developed by introducing hydrophobic and/or hydrophilic groups to the chitosan backbone and has been used as the delivery vehicles for gene [22], peptide [23], and antitumor drugs [11,24]. The chitosan-based amphiphiles can form micelles by self-assembly in water. In our previous reports [11,25], we synthesized a series of novel water-soluble chitosan derivatives carrying long chain alkyl groups ($n = 8$, 10, 12) as hydrophobic moieties and sulfated groups as hydrophilic moieties for the solubilization of PTX, and among them *N*-octyl-*O*-sulfate chitosan (NOSC) showed the highest capacity in solubilizing PTX. The solubility of PTX in micelle systems formed by NOSC was up to 2.6 mg/mL, which was a 1000 times higher than that of the saturated concentration of PTX in water.

The primary aim of the present study is to further evaluate and compare the pharmacokinetics, biodistribution, antitumor efficacy and safety of PTX-loaded NOSC micelles (PTX-M) and Taxol. The comparable antitumor efficacy of PTX-M and Taxol® was observed at the same dose of 10 mg/kg, but PTX-M significantly improved bioavailability and reduced toxicity.

2. Materials and methods

2.1. Materials

Chitosan was purchased from the Suanglin Biochemical Co. Ltd. (Nantong, China), with deacetylation degrees of 92% and viscosity average molecular weight of 65 kDa. PTX was provided by Taihua Natural Plant Pharmaceutical Co. Ltd. (Shanxi, China). Docetaxel (99.5%) was a gift from Junjie Biotechnology Co. Ltd. (Shanghai, China). Diazepam was obtained from Nanjing Xiandao Chemical Co. Ltd. (Jiangsu, China). *N*-octyl-*O*-sulfate chitosan (NOSC) was synthesized using the chitosan mentioned above by our group, and the substitution of octyl degree and sulfonic degree were 0.38 and 2.56 and viscosity average molecular weight was 65–70 kDa, respectively. The values of octyl degree, sulfonic degree and viscosity average molecular weight of NOSC were stable, and good batch-to-batch reproducibility of the NOSC was ensured.

HPLC/spectra-grade reagents were used as the mobile phase in HPLC analysis, and all other reagents were analytical grade and used without further purification. Distilled and deionized water was used in all experiments.

2.2. Animals

Sprague-Dawley (SD) rats were obtained from the Shanghai Silaike Laboratory Animal Limited Liability Company. Kunming mice were obtained from New Drug Screening Center of China Pharmaceutical University, C57 mice and BALB/cA nude mice were obtained from Shanghai Institute of Materia Medica of Chinese Academy of Sciences. New Zealand albino rabbits (1.8–2.0 kg) and guinea pigs (280–330 g) were obtained from the Laboratory Animal Center of Nanjing General Hospital. All the animals were pathogen free and allowed to access food and water freely. The experiments were carried out in compliance with the National Institute of Health Guide for the Care and Use of Laboratory Animals.

2.3. Preparation of PTX-M

PTX-M was prepared by dialysis as described previously [11]. Briefly, the orthogonal design was used to optimize the preparation of PTX-M. PTX (12.5 mg) and NOSC (12.0 mg) were dissolved in 0.2 mL of dehydrated ethanol and 2.0 mL of distilled water, respectively, and both solutions were cooled down on ice for a few minutes. The PTX solution was added into the NOSC solution drop by drop with constant stirring. The mixed solution was subject to dialysis against 2 L deionized water at 0 °C for 6 h. The micelle solution was filtrated through a 0.45 μm pore-sized membrane and lyophilized by a freeze dryer system (Yuhua, China) to obtain the dried powder of PTX-M. The hydrodynamic diameter and Zeta potential of the micelles were measured by dynamic light scattering (Zetasizer 3000 HAS, Malvern, UK) at a polymer concentration of 6 mg/mL.

An aliquot of PTX-M was treated with 50 times volume of methanol to disrupt the micelle structure. The amount of encapsulated PTX was measured using a reverse-phase HPLC method. The stock solution of PTX (1.0 mg/mL) was prepared by dissolving 50.0 mg of PTX into 50.0 mL of methanol, and standard curve was set up with satisfactory linearity. The HPLC system consisted of a HP1050 series (Agilent Technologies, Palo Alto, CA, USA) was used. Chromatographic separations were achieved using a Lichrospher C18 column (4.6 × 250 mm, Hanbon, Jiangsu, China) at 40 °C. The mobile phase consisted of deionized water and HPLC grade methanol [25:75 (V/V)]. The samples were delivered at a flow rate of 1.0 mL/min and detected at 227 nm using UV detection (Agilent Technologies, Palo Alto, CA, USA).

2.4. Pharmacokinetic studies

Sprague-Dawley rats (220–260 g) were used to examine the pharmacokinetics of PTX-M. Rats were randomly divided into following four groups ($n = 6$): (1) PTX-M (3.5 mg/kg); (2) PTX-M (7 mg/kg); (3) PTX-M (14 mg/kg); and (4) Taxol® (7 mg/kg). Drugs were intravenously administrated through the tail vein. The blood samples (0.5 mL) were collected from the plexus venous in the eyeground at 1 min, 5 min, 10 min, 30 min, 1 h, 2 h, 3 h, 4 h, and 8 h. The plasma was obtained by centrifugation at 6000 rpm for 10 min and stored at −20 °C. The PTX concentrations were determined by HPLC. Drug and Statistics for Windows (DAS ver1.0) was utilized to analyze the pharmacokinetic parameters of the area under the plasma concentration–time curve ($AUC_{0-\infty}$), the apparent volume of distribution (V_d), total body clearance (CL), elimination half life ($t_{1/2\beta}$) and mean residence time (MRT) of PTX for each formulation. Appropriate models fitting the plasma

concentrations data were evaluated by criteria according to the goodness of fit for each model. Especially, Akaike's Information Criterion (AIC) Rule was observed in the determination of the appropriate compartment model. The goodness of fit for each model was distinguished by the value of AIC, the optimum compartment model was determined with minimum AIC value. If there was no significant difference between the optimum compartment model and suboptimum compartment model, the simple compartment model was selected as appropriate compartment model.

2.5. Biodistribution

To assess the effect of micelle formulation on tissue distribution of PTX, rats (50% male and 50% female) were randomly divided into two groups ($n = 24$), Taxol® and PTX-M. Taxol® and PTX-M were intravenously administrated via tail vein at a dose of 7 mg/kg. After injection, rats were exsanguinated through femoral artery at 15 min, 1 h, 4 h and 8 h after drug administration (six rats for each time point). The blood, heart, liver, spleen, lung, kidney, stomach, intestine, genitals, brain, muscle, and spinal cord were collected. Tissue samples were blotted with paper towel, rinsed in saline, blotted to remove excess fluid, weighed and stored at −20 °C.

2.6. Measurement of PTX levels in plasma and tissue samples by HPLC

Plasma concentrations of PTX were determined by reverse-phase HPLC with UV detection [25]. Briefly, 200 μl of plasma and 50 μL of internal standard (diazepard) were extracted twice with 0.8 mL of tetra-butyl methyl ether. The total organic layer was separated by centrifugation at 6000 rpm for 10 min, and transferred to a clean tube. The drug residue was obtained by evaporation and reconstituted in a methanol–water (65:35, V/V) solution. After centrifugation at 14,000 rpm for 10 min, 20 μL aliquots of the supernatant were injected into the HPLC system.

Tissue concentrations of PTX were determined by reverse-phase HPLC/MS/MS as described previously [26]. Briefly, tissue samples were homogenized (Tearork™, BioSpec Products Inc., Bartlesville, OK) in saline. The homogenate (0.7 mL) was mixed with 50 μL of internal standard (docetaxel, 25 μg/mL) and extracted with 3.5 mL of tetra-butyl methyl ether twice. The drug residues were obtained as described above and reconstituted in 200 μL of a solution containing methanol–water–methanoic acid (77:23:0.115). Aliquots of 25 μL were injected into the HPLC/MS/MS system.

The HPLC/MS/MS system (Alliance 2695-Quattro micro API, Waters, USA) was equipped with electrospray ionization (ESI) source (San Jose, CA, USA), a Finnigan surveyor LC pump and an autosampler. Data acquisition was performed with Quanlynx software (Thermo-Finnigan, San Jose, CA, USA). Peak integration and calibration were carried out using LC Quan software (Thermo-Finnigan).

A Lichrospher C18 column (4.6 × 150 mm, Hanbon, Jiangsu, China) with a mobile phase of water, methanol and methanoic acid (23:77:0.115) was used for chromatographic separations. The flow rate and column temperature were set at 1 mL/min and 30 °C, respectively. Mass spectrometric analysis was performed in the positive ion mode (ESI+) and set up in the multiple reaction monitoring (MRM) modes. The capillary temperature was 100 °C, and the spray voltage was 3000 V. Collision induced dissociation (CID) studies were performed and argon was used as the collision gas with its pressure of 1.9 MPa. The collision energy was 20 eV.

2.7. In vivo antitumor efficacy

In vivo antitumor efficacy of PTX-M was evaluated with the animal tumor models set up by inoculation of sarcoma180, Ehrlich solid carcinoma (EC), hepatoma solidity (Heps), Lewis lung cancer or A-549 human lung cancer, respectively.

Kunming mice (18–22 g, 50% male and 50% female) were injected subcutaneously in the armpit of right anterior limb with 0.2 mL of cell suspension containing one of the three kinds of sarcoma180, Ehrlich solid carcinoma (EC), hepatoma solidity (Heps). After 24 h (day 0), mice were weighed and randomly divided into five groups ($n = 10$): (1) negative control group (saline group); (2) positive control group (Taxol, 10 mg/kg); (3) PTX-M (2.5 mg/kg); (4) PTX-M (5 mg/kg); and (5) PTX-M (10 mg/kg). The control saline or drugs were administrated via tail vein at day 0, day 2, day 4 and day 6. At day 8, all the mice were weighted and sacrificed by cervical vertebra dislocation following by separation and measurement of the tumor block. The antitumor efficacies of each formulation were evaluated by tumor inhibition rate, which was calculated by the following formula: ((tumor weight − tumor weight of negative control group)/tumor weight of negative control group × 100%).

The therapeutic effect of PTX-M was estimated using female BALB/cA nude mice model (5–6 weeks, 18–22 g), which was inoculated subcutaneously with 1×10^6 A-549 human lung cancer cell line. Treatments were started when tumor in the nude mice reached a tumor volume of 100–300 mm^3, this day was designated day 0. On day 0, mice were randomly divided into negative control group ($n = 12$), positive Taxol control group ($n = 6$) and three PTX-M groups ($n = 6$). Control saline or Taxol (10 mg/kg) or PTX-M (2.5, 5 or 10 mg/kg) was injected intravenously via tail vein three times a week. Tumor size was measured twice per week during the study. Tumor volume was calculated by the formula: $(W^2 \times L)/2$, where W is the tumor measurement at the widest point, and L is the tumor dimension at the longest point. Relative tumor volume (RTV) was calculated by the formula: V_i/V_0, where V_0 is the tumor volume at day 0, and V_i is the tumor volume at the measurement point. Antitumor activity was estimated by relative tumor growth rate (T/C (%)) which was calculated by the formula: [RTV (treatment group)/RTV (negative control group)] × 100%.

2.8. Intravenous injection safety assessment

2.8.1. Acute toxicity of PTX-M

To determine the acute toxicity of PTX-M, the LD_{50} of both PTX-M and Taxol® were calculated and the toxic effects on major organs were examined. Kunming mice (half male and half female, 18–22 g) were housed under normal conditions with free access to food and water. Mice were randomly divided into five groups ($n = 10$), and the freeze-dried power of PTX-M was re-dissolved in 5% glucose injection solution and injected via tail vein at the dose of 53, 66, 83, 104, and 130 mg/kg, respectively. Mice were observed for 2 weeks in all groups, and the number of mice surviving was recorded. The LD_{50} was calculated using the Bliss method.

The LD_{50} of Taxol® was calculated in the same way as described above as control group, while the doses were 32.8, 41, 51.2, 64, and 80 mg/kg, respectively.

2.8.2. Hemolysis test

Rabbit blood was used to test the Hemolysis effect of PTX-M. Briefly, 10 mL of rabbit blood was obtained from arteria cruralis and the fibrinogen was removed by stirring with glass rod. Ten milliliter of 5% glucose injection solution was added into defibrinogen blood sample, and supernatant was removed after centrifugation at 3000 rpm for 5 min. The erythrocyte pellets at the bottom of centrifuge tube were washed four times (centrifugation followed by re-dispersion) with 5% glucose injection solution. Finally, after repeated washing and centrifugation, an adequate amount of 5% glucose injection was added to the erythrocyte pellets to give a 2% erythrocyte standard dispersion and stored at 4 °C. The lyophilized power of PTX-M was dissolved in 5% glucose injection solution at a concentration of 0.25 mg/mL, and different amounts of micelle solution with volume of 0, 0.1, 0.2, 0.3, 0.4 and 0.5 mL were added into six tubes with 2.5 mL of 2% erythrocyte dispersion in each. Then adequate amounts of 5% glucose injection solution were added in every tube to obtain a final volume of 5 mL. Positive control was prepared by addition of 2.5 mL of water into 2.5 mL of 2% erythrocyte dispersion instead of 5% glucose injection and micelle solution. After vortex, the tubes were incubated at 37 °C and observed microscopically from 15 min to 4 h.

2.8.3. Intravenous irritation assessment

One male and two female rabbits weighing 1.8–2.0 kg were used for this study. PTX-M was dissolved in 5% glucose injection solution at the concentration of 0.33 mg/mL. Each rabbit was injected with a daily dose of 6 mg/kg of micelle solution into the vein at the edge of the left ear at an injection

rate of 1 mL/min for 3 days. And equivalent volume of 5% glucose injection solution was injected into the right ear-border vein meanwhile as control. After injection, paradoxical reaction at the injection site was recorded. The rabbits were sacrificed by blood letting 24 h after the last administration, and the ears were cut and fixed in 10% liquor formaldehyde for histological examination. At the localizations of 1.3, 2.6 and 4.0 cm from the injection site to proximal part, histological sections were prepared for histopathological examination.

2.8.4. Injection anaphylaxis

Guinea pigs (220–270 g) were randomly assigned to following three groups ($n = 6$, 50% male and 50% female): (1) negative control group; (2) positive control group; and (3) PTX-M group. Animals were intraperitoneally injected every other day with 5% glucose injection solution for negative control group, 4% egg albumen solution for positive control group and PTX-M solution (2.0 mg/mL in 5% glucose injection) for PTX-M group. After the third injection, each group was further divided into two sub-groups ($n = 3$). Animals in sub-group one were intraperitoneally injected with corresponding agent 14 days after the first injection; animals in sub-group two were intraperitoneally injected with corresponding agent 21 days after the first injection. The anaphylactic response was recorded 30 min after last injection.

2.9. Statistical analysis

Statistical analysis was performed by Student's *t*-test for two groups, and one-way ANOVA for multiple groups. All results were expressed as the mean ± standard deviation (SD) unless otherwise noted. A probability (p) of less than 0.05 is considered statistically significant.

3. Results

3.1. Characterization of PTX-M

We have previously revealed the efficient encapsulation of PTX in NOSC micelles by using a dialysis method [11]. The drug loading and entrapment efficiency could reach 25.25% and 59.11%, respectively. The micelle size and polydispersity were around 240 nm and 0.35, respectively, which were measured by dynamic light scattering. According to the orthogonal design, we optimized the conditions to prepare PTX-M. The optimal feed ratio of NOSC and PTX was screened as 12/12.5 (W/W), and the temperature of dialysis water was controlled at 0 °C, besides, sonication and centrifugation were rejected, the resultant drug loading and entrapment efficiency increased obviously, achieving 60.91% and 97.26%, respectively. The micelle size reduced to around 200.8 nm with the polydispersity of 0.31. The empty micelles were negatively charged with Zeta potential of approximately −31.1 mV, while micelles loading with PTX slightly decreased the negativity of the micelles to −28.8 mV. This also revealed that the negatively charged hydrophilic sulfonic group was located on the surface of micelles.

3.2. Pharmacokinetics of PTX-M after intravenous administration

The drug concentration was detected by HPLC analysis, which has been validated. The plasma concentration–time profiles of PTX after i.v. administration of PTX-M and Taxol® were shown in Fig. 1. The pharmacokinetic parameters of PTX in the two formulations after i.v. administration at three dosages were shown in Table 1. For PTX-M, the values of area under the plasma concentration–time curve ($AUC_{0-\infty}$) for three different doses, 3.5, 7 and 14 mg/kg were 1019.7, 3009.9 and 7252.6 μg/L/h, respectively; whereas the corresponding total body clearance (CL) were 2.91, 2.49 and 1.99 L/kg, respectively. A rapid decline in concentrations of PTX in micelle group represented a distribution phase, which was followed by an elimination phase with $t_{1/2\beta}$ of 2.93, 2.15 and 1.69 h, respectively. Both PTX-M and Taxol® displayed the similar distribution trends at the same dose of 7 mg/kg (Fig. 1). However, the plasma AUC of PTX-M was 3.6-fold lower than that of the Taxol®; and the V_d, $t_{1/2\beta}$ and CL of PTX in PTX-M were increased by 5.7, 1.65 and 3.5-fold, respectively.

3.3. Tissue distribution of PTX-M after intravenous administration

The tissue distribution profiles of PTX-M and Taxol® after intravenous administration were compared in rats. The

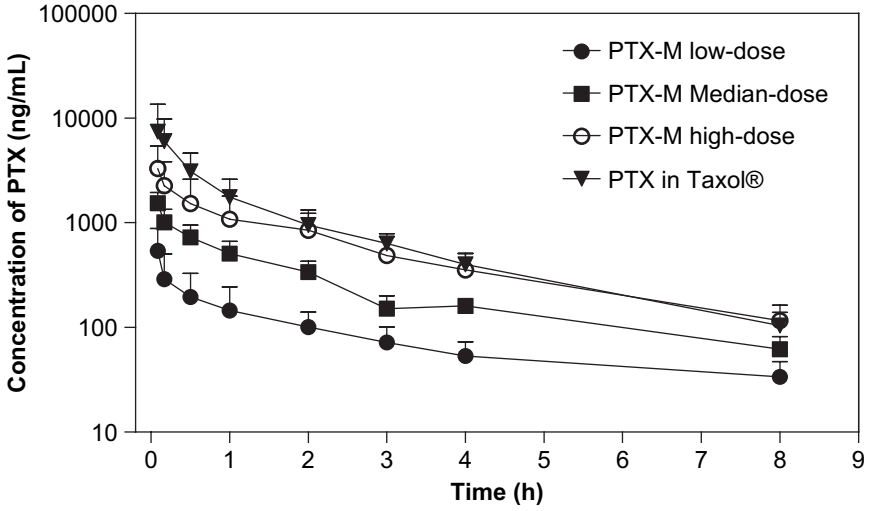

Fig. 1. Time courses of PTX levels in rat plasma after i.v. administration of PTX-M and Taxol®. Each point represents the mean ± SD ($n = 6$).

Table 1
Pharmacokinetic parameters of PTX in the two formulations after i.v. administration at three dosages

Drug and dose (mg/kg)	PTX-M			Taxol®
	3.5	7	14	7
V_d (L/kg)[a]	12.3 ± 8.0	7.06 ± 2.89***	4.71 ± 1.40	1.23 ± 0.14
$t_{1/2\alpha}$ (h)[b]	0.133 ± 0.110	0.237 ± 0.183	0.0891 ± 0.0602	0.157 ± 0.068
$t_{1/2\beta}$ (h)[c]	2.93 ± 1.45	2.15 ± 1.03	1.69 ± 0.45	1.30 ± 0.41
$AUC_{0-\infty}$ (μg/L/h)[d]	1019.7 ± 256.1	3009.9 ± 877.1***	7252.6 ± 1929.3	10,714.2 ± 3514.8
CL (L/h/kg)[e]	2.91 ± 1.25	2.49 ± 0.98*	1.99 ± 0.53	0.715 ± 0.257
$MRT_{0-\infty}$ (h)[f]	2.28 ± 0.28	2.03 ± 0.25**	1.97 ± 0.22	1.41 ± 0.26

Data represent mean value ± SD, $n = 6$.
*$p < 0.05$, **$p < 0.01$, ***$p < 0.001$, compared with Taxol®.
[a] V_d, apparent volume of distribution.
[b] $t_{1/2\alpha}$, distribution half life.
[c] $t_{1/2\beta}$, elimination half life.
[d] $AUC_{0-\infty}$, area under the plasma concentration–time curve.
[e] CL, total body clearance.
[f] MRT, mean residence time.

concentration of PTX in each tissue was determined by HPLC analysis. As shown in Fig. 2, PTX was widely and rapidly distributed into most tissues following i.v. administration of micellar preparation, and the highest concentration of PTX was found in liver, followed by kidney and lung at 15 min after administration. However, after 8 h, the drug concentration was decreased in the following order: spleen > liver > lung > kidney; and PTX concentrations in spinal cord and brain were very low.

3.4. In vivo antitumor efficacy

In vivo antitumor efficacy of PTX-M was evaluated with the animal tumor models set up by inoculation of sarcoma180,

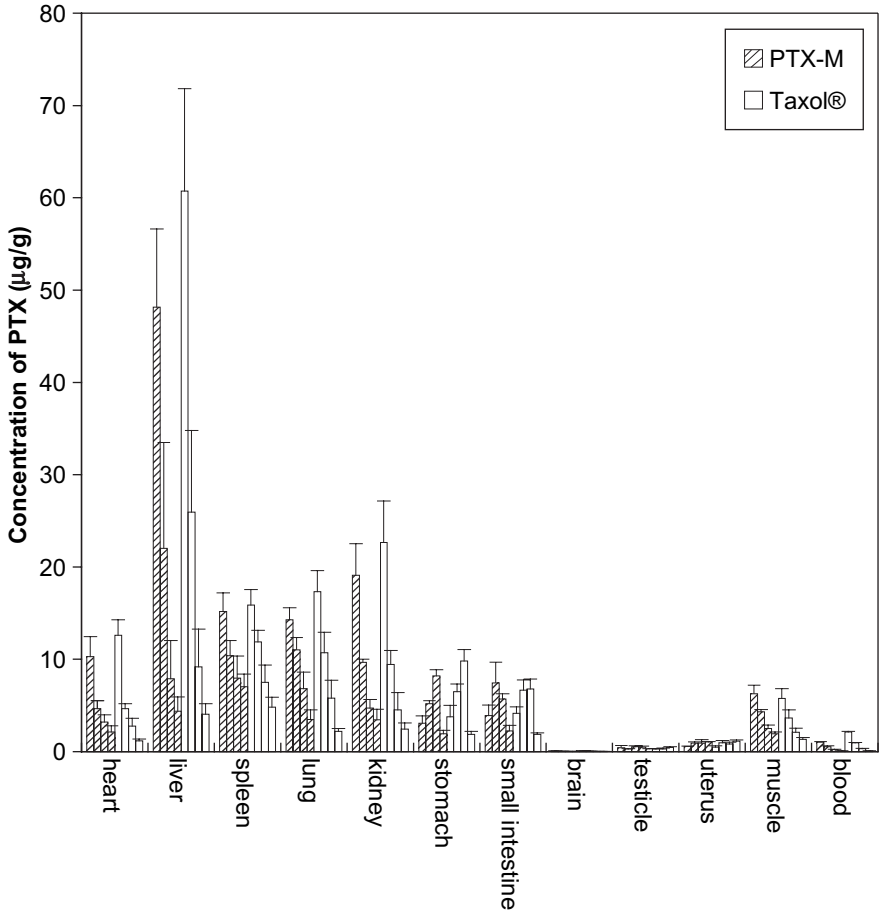

Fig. 2. Comparison of PTX concentrations in rats receiving PTX-M (hatched columns) or Taxol® (blank columns) at a dose of 7 mg/kg at different sample times (in the order of 15 min, 1 h, 4 h and 8 h). Each column represents the mean ± SD ($n = 6$).

Ehrlich solid carcinoma (EC), hepatoma solidity (Heps), Lewis lung cancer or A-549 human lung cancer, as described in methods.

The antitumor effect of PTX-M was compared with that of Taxol® by measuring tumor weight of mice or relative tumor growth rate of nude mice after tumor implantation. As shown in Table 2, PTX-M markedly inhibited the growth of sarcoma180 and Ehrlich solid carcinoma (EC), Lewis lung cancer at doses of 5 and 10 mg/kg ($p < 0.01$) and modestly inhibited the growth of hepatoma solidity (Heps) at 10 mg/kg ($p < 0.01$). In contrast, Taxol® had no significant inhibitory effect on the growth of Heps at dose of 10 mg/kg ($p > 0.05$). Taxol® displayed the similar tumor inhibition rates as PTX-M at the dose of 10 mg/kg to all of the tested tumors except Heps. Similarly, the comparable therapeutic effects on A-549 human lung cancer cell bearing BALB/cA nude mice were observed by treatment with PTX-M and Taxol® at the same dose of 10 mg/kg, and the *T/C* (%) were 46.8–52.5 and 46.1–50.9, respectively. However, the toxic effects (body weight loss) was only observed in Taxol® group but not in PTX-M groups at all doses.

3.5. Injection safety

3.5.1. Acute toxicity of PTX-M

The median lethal dose (LD_{50}) was used to determine the acute toxicity as described in methods. Mice were injected with various doses of PTX-M or Taxol® via the lateral vein tail or intraperitoneal once. The toxic response such as severe prostration, apathy, respiratory distress, and catatonia were observed and several mice died after 24 h. The main organs of dead mice, such as heart, liver, spleen, lung, and kidney, were subject to macroscopic examination. No obvious changes were observed. After 7 days of dosing, the survivors were gradually recovered. The dose–toxicity relationship observed on day 7 was shown in Fig. 3. The LD_{50} of PTX-M administered by intravenous injection and intraperitoneal injection was 72.16 and 81.28 mg/kg, respectively, and the 95% confidence limits were found to fall in the range of 67.65–76.97 and 73.65–89.70 mg/kg, respectively. The corresponding LD_{50} of the Taxol® was 49.09 and 53.43 mg/kg, respectively, which was 1.47–1.52-folds lower than that of PTX-M. The corresponding 95% confidence limits were calculated as 43.50–55.40 and 47.51–60.09 mg/kg, respectively. These parameters indicated that the PTX-M is less toxic than Taxol® and provided critical guidelines for the administration of PTX-M in future studies.

3.5.2. Hemolysis test

Complete hemolysis was observed in tube of positive control at 15 min, the solution was red clear-diaphanous, and no erythrocyte survived at the bottom of the tube. The erythrocyte precipitated at the bottom of other six tubes and dispersed after

Table 2
In vivo antitumor effect of PTX-M and Taxol® in tumor bearing mice model

Tumor model	Drug	Dose (mg/kg)	Body weight (g)		Tumor weight (g)
			Before administration	After administration	
Sarcoma180	PTX-M	2.5	19.8 ± 1.33	27.0 ± 1.48	1.15 ± 0.14
		5	19.6 ± 1.43	26.2 ± 1.78	0.91 ± 0.32**
		10	19.7 ± 1.42	25.4 ± 0.92*	0.73 ± 0.25**
	Taxol®	10	19.9 ± 1.30	24.0 ± 1.10**	0.80 ± 0.18**
	Normal saline	0.2 mL/mouse	19.7 ± 1.49	27.6 ± 2.01	1.09 ± 0.20
Ehrlich solid carcinoma	PTX-M	2.5	19.8 ± 1.66	26.8 ± 1.72	1.01 ± 0.32*
		5	19.6 ± 1.56	25.9 ± 1.45	0.91 ± 0.22**
		10	19.4 ± 1.20	25.3 ± 1.42*	0.70 ± 0.23**
	Taxol®	10	19.9 ± 1.37	24.3 ± 0.9**	0.77 ± 0.24**
	Normal saline	0.2 mL/mouse	19.8 ± 1.47	27.1 ± 1.45	1.33 ± 0.33
Hepatoma solidity	PTX-M	2.5	19.3 ± 1.19	27.6 ± 2.06	1.05 ± 0.21
		5	19.3 ± 1.42	26.1 ± 1.70	0.95 ± 0.33
		10	19.2 ± 1.08	25.6 ± 1.02	0.71 ± 0.15*
	Taxol®	10	19.9 ± 1.30	24.5 ± 1.5*	0.87 ± 0.19
	Normal saline	0.2 mL/mouse	19.7 ± 0.90	27.9 ± 3.01	1.19 ± 0.34
Lewis lung cancer	PTX-M	2.5	19.6 ± 1.58	24.6 ± 0.84	1.22 ± 0.33
		5	19.8 ± 1.48	24.3 ± 1.16	0.96 ± 0.18**
		10	20.1 ± 1.60	23.9 ± 1.29	0.66 ± 0.17**
	Taxol®	10	19.9 ± 1.52	22.7 ± 1.25**	0.67 ± 0.15**
	Normal saline	0.2 mL/mouse	19.8 ± 1.48	24.7 ± 1083	1.48 ± 0.32

Tumor model	Drug	Dose (mg/kg)	Body weight (g)		TV (mm^3)	
			Before administration	After administration	Before administration	After administration
A-549 human lung cancer	PTX-M	2.5	21.4 ± 1.50	23.2 ± 0.9	117 ± 25	764 ± 288
		5	20.2 ± 1.40	22.8 ± 1.40	117 ± 32	546 ± 240*
		10	20.9 ± 0.40	23.1 ± 0.5	112 ± 25	477 ± 162*
	Taxol®	10	21.3 ± 1.10	22.0 ± 0.90	123 ± 21	501 ± 123*
	Normal saline	0.2 mL/mouse	20.6 ± 0.90	23.0 ± 1.30	112 ± 46	885 ± 338

Data represent mean value ± SD, $n = 50$.
*$p < 0.05$, **$p < 0.01$, compared with Normal saline group.

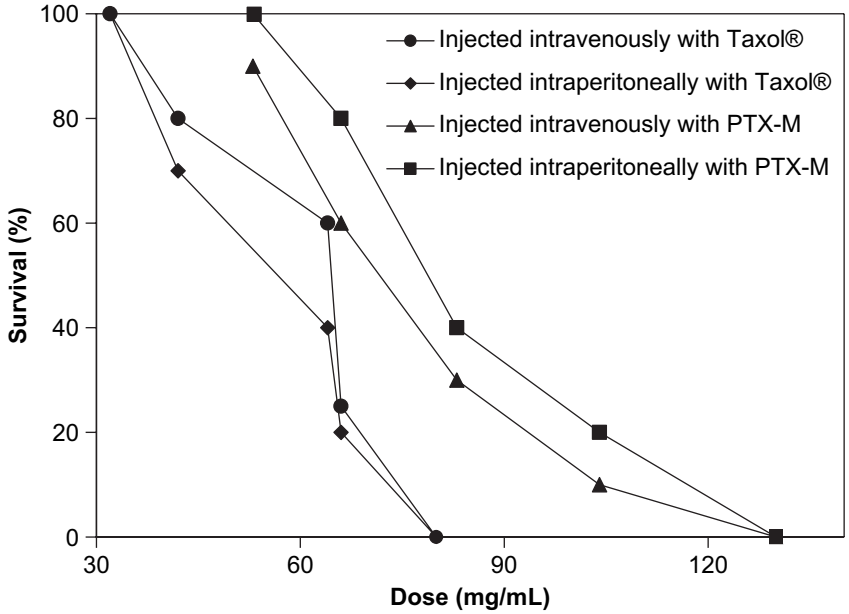

Fig. 3. Acute toxicity of PTX-M and Taxol® injected intravenously and intraperitoneally. The percentage survival at day 7 is shown.

shaking, and the supernatant was achromatic and transparent in the observation period for 4 h. These results demonstrated that the PTX-M solution at concentration of 0.025 mg/mL did not cause haematolysis and erythrocyte agglutination at 37 °C.

3.5.3. Intravenous irritation

After a 3-day administration of PTX-M solution and 5% glucose injection, erythema and edema were not observed at the injection sites. The histopathologic examination of the rabbit ear-border vein indicates that the vessel wall and endothelial cell structures were unimpaired. Furthermore, angiectasia and thrombus were not observed in the lumen of vein. There were no significant pathological changes, inflammatory cell infiltrate, hemorrhage apomorphosis and necrosis in the vessel wall and surrounding tissues. The histopathologic examination results of the rabbit ears administrated with micelle solution were similar to that of the control group. All the results demonstrated that PTX-M solution at a dose of 6 mg/kg has no simulative reaction in the ear vein of rabbit.

3.5.4. Injection anaphylaxis

Positive reaction was assessed with the occurrence of the behaviors such as convulsion, collapse, circulatory collapse and death or occurrence of at least two kinds of anaphylactic response such as piloerection, anhelation, sneeze, retch, and begma. The results demonstrated that PTX-M treated group and negative control group did not respond to the last challenge. However, in positive control, typical anaphylaxis, such as anhelation and convulsion, occurred immediately after last challenge, and all the three guinea pigs died within 1 min. These results demonstrated that the PTX-M solution used intravenously at concentration of 2.0 mg/mL did not cause hypersensitivity.

4. Discussion

Orthogonal design was used to optimize the preparation of PTX-M, unemployment of centrifugation increased the loading and entrapment efficacy enormously, second by the adjustment of feeding ratio of NOSC and PTX, and the lower temperature of dialysis water was in favor with the minimized particle size and polydispersity. The micelle size reduced to around 200.8 nm with the polydispersity of 0.305 after modification. The empty micelles were negatively charged with Zeta potential of approximately −31.1 mV, while micelles loading with PTX slightly decreased the negativity of the micelles to −28.8 mV. The polydispersity demonstrated a wide size distribution of the micelle particle, and micelle size exceed 200 nm might not avoid recognition of RES [27]. Although PTX was widely distributed into most tissues following i.v. administration of micelle preparation, the most of PTX were found in the liver, kidney, spleen, and lung. These were agreeing with the results reported by Rowinsky and Donehower [28], and the localization of PTX in the liver, spleen and lungs was consistent with the uptake by the RES. Particulates with an average size below 7 μm were generally taken up by the Kupffer cells of liver and macrophages of the spleen [29] and alveolar macrophages in the lungs [30].

In addition, Zeta potential can greatly influence the particle stability in suspension through the electrostatic repulsion between the particles. The particles repel each other and the colloid is stable with the high charge and if the charge is near zero, Brownian movement causes the particle to collide and attach each other. It is desirable to maximize the particle charge in order to achieve greatest stability.

The decline in plasma concentrations could be described by a two-compartment open model. As indicated in Table 1, the

dose of PTX in PTX-M was escalated from 3.5 to 14 mg/kg, the plasma AUC increased from 1019.7 to 7252.6 μg/L/h, a 4-fold increase in the dose level of PTX-M resulted in a non-liner 7.11-fold increase in the plasma AUC. The calculated terminal half life ($t_{1/2\beta}$) decreased over-proportionally with the increase of the dose. These results indicated a non-linear pharmacokinetic behavior of PTX-M in rats. And upon dose escalation, both the over-proportional increase in AUC and decrease in CL were consistent with saturable processes of elimination and distribution of PTX, which were observed when the plasma concentration of the drug was above a ''saturation point'' [31]. The influence of pharmaceutical vehicle NOSC on the pharmacokinetics behavior of PTX in rats paralleled the effects of Cremophor EL in Taxol®. It had reported that the non-linear pharmacokinetics of PTX in mice resulted from the pharmaceutical vehicle Cremophor EL. In our research of PTX-M in rats by i.v. administration, the similar phenomenon was observed. Although lots of presumption was proposed, the relationship between Cremophor EL and the pharmacokinetics of PTX was still poorly understood [32]. The change in the biological fate of PTX, imposed by its encapsulation in NOSC micelles, had led to a decrease in AUC as a result of an increase in CL and V_d for the encapsulated drug.

The results obtained from tissue distribution study of PTX-M by i.v. administration were also consistent with the results reported by Rowinsky and Donehower [28]. The localization of PTX in the liver, spleen and lungs was consistent with the uptake by RES. However, a considerable amount of PTX was also accumulated in some non-RES organ, such as kidney, suggesting that other factors (blood perfusion of the organ) in addition to the uptake by RES system may also affect the tissue specificity of the micelles. Although PTX-M and Taxol® had the similar effects on PTX accumulation in lung, but the retention time of PTX-M in lung was longer. This may due to the nature of chitosan, which was easy to adhere to the vascular wall and mucosa. PTX-M may be detained in the lung and release the drug continuously, which is propitious to the therapy of non-small cell lung cancer. In addition, the peak concentrations of both formulations in non-gastrointestinal tissues (heart, lung, liver, spleen, and kidney) were reached at 15 min, but the peak concentrations in stomach and small intestine were reached at latter sample time. Similar result was obtained in Yeh's study [33], which may due to the excretion of PTX into the gastrointestinal tract.

The in vivo antitumor studies indicate (Table 2) that PTX-M and Taxol® had the similar antitumor efficacy at the same dose of 10 mg/kg. But the toxic effect of PTX-M was much less than that of Taxol®. PTX-M did not cause weight loss. The LD_{50} of PTX-M were 1.47–1.52-folds higher than that of Taxol®, which further indicated the lower toxicity of PTX-M than Taxol®. Taken together, these studies demonstrated that PTX-M had the similar to better therapeutic effects as Taxol® on various tumors, but significantly reduced the toxic effects associated with Taxol®.

5. Conclusion

In summary, a micelle delivery system based on *N*-octyl-*O*-sulfate chitosan was developed and characterized as an effective alternative to Cremophor EL and dehydrated alcohol as the delivery system for PTX. Pharmacokinetic and pharmacological studies demonstrated that PTX-M had the similar antitumor efficacy as Taxol®, but significantly reduced the toxic effects and improved the bioavailability of PTX. These results indicate that NOSC micelles overcome the disadvantages of conventional delivery systems containing Cremophor EL and dehydrated alcohol and appear to be the best possible approach which would bypass the limitations of current delivery system and provide a desirable therapeutic efficacy.

Acknowledgements

This study is financially supported by the National 863 project (2004AA2Z3232), the key program of international science & technology research cooperation (2005DFA30350) of the State Ministry of Science & Technology of China, Natural Science Foundation of Jiangsu, China (BK2006154), Program for New Century Excellent Talents in University (NCET-06-0499), National Natural Science Foundation of China (30772662) and Natural Science Foundation of Jiangsu, China (BK2006154).

References

[1] Panchagnula R. Pharmaceutical aspects of PTX. Int J Pharm 1998;172:1–15.
[2] Rowinsky EK, Cazenave LA, Donehower RC. Taxol: a novel investigational antimicrotubule agent. J Natl Cancer Inst 1990;82:1247–59.
[3] Wall EM, Wan MC. Camptothecin and Taxol: discovery to clinic. Cancer Res 1995;55:753–60.
[4] Szebeni J, Muggia FM, Alving CR. Complement activation by Cremophor EL as a possible contributor to hypersensitivity to PTX: an in vitro study. J Natl Cancer Inst 1998;90:300–6.
[5] Fonseca C, Simoes S, Gaspar R. PTX-loaded PLGA nanoparticles: preparation, physicochemical characterization and in vitro anti-tumoral activity. J Control Release 2002;83:273–86.
[6] Crosasso P, Ceruti M, Brusa P, Arpicco S, Dosio F, Cattel L. Preparation, characterization and properties of sterically stabilized PTX-containing liposomes. J Control Release 2000;63:19–30.
[7] Sharma US, Balasubramanian SV, Straubinger RM. Pharmaceutical and physical properties of PTX (Taxol) complexes with cyclodextrins. J Pharm Sci 1995;84:1223–30.
[8] Kan P, Lin XZ, Hsieh MF, Chang KY. Thermogelling emulsions for vascular embolization and sustained release of drugs. J Biomed Mater Res B Appl Biomater 2005;75:185–92.
[9] Skwarczynski M, Noguchi M, Hirota S, Sohma Y, Kimura T, Hayashi Y, et al. Development of first photoresponsive prodrug of PTX. Bioorg Med Chem Lett 2006;16:4492–6.
[10] Kim SC, Kim DW, Shim YH, Bang JS, Oh HS, Kim SW, et al. In vivo evaluation of polymeric micellar PTX formulation: toxicity and efficacy. J Control Release 2001;72:191–202.
[11] Zhang C, Ping QN, Zhang HJ. Self-assembly and characterization of PTX-loaded *N*-octyl-*O*-sulfate chitosan micellar system. Colloids Surf B Biointerfaces 2004;39:69–75.
[12] Aliabadi HM, Lavasanifar A. Polymeric micelles for drug delivery. Expert Opin Drug Deliv 2006;3:139–62.

[13] Kwon GS, Okano T. Polymeric micelles as new drug carriers. Adv Drug Deliv Rev 1996;21:107–16.
[14] Muzzarelli RAA, Muzzarelli C. Chitosan chemistry: relevance to the biomedical sciences. Adv Polym Sci 2005;186:151–209.
[15] Calvo P, Remunan C, Vila JL, Alonso MJ. Chitosan and chitosan ethylene oxide propylene oxide block copolymer nanoparticles as novel carriers for proteins and vaccines. Pharm Res 1997;14:1431–6.
[16] Rege PR, Shukla DJ, Block LH. Chitinosans as tableting excipients for modified release delivery systems. Int J Pharm 1999;181:49–60.
[17] Mi FL, Shyu SS, Kuan CY, Lee ST, Lu KT, Jang SF. Chitosan-polyelectrolyte complexation for the preparation of gel beads and controlled release of anticancer drug. I. Effect of phosphorous polyelectrolyte complex and enzymatic hydrolysis of polymer. J Appl Polym Sci 1999; 74:1868–79.
[18] Tomihata K, Ikada Y. In vitro and in vivo degradation of films of chitin and its deacetylated derivatives. Biomaterials 1997;18:567–75.
[19] Hirano S, Zhang M, Nakagawa M, Miyata T. Wet spun chitosan–collagen fibers, their chemical *N*-modifications, blood compatibility. Biomaterials 2000;21:997–1003.
[20] Rege PR, Garmise RJ, Block LH. Spray-dried chitinosans. Part II: in vitro drug release from tablets made from spray-dried chitinosans. Int J Pharm 2003;252:53–9.
[21] Ravi Kumar MNV, Muzzarelli RAA, Muzzarelli C, Sashiwa H, Domb AJ. Chitosan chemistry and pharmaceutical perspectives. Chem Rev 2004;104:6017–84.
[22] Hu FQ, Zhao MD, Yuan H. A novel chitosan oligosaccharide–stearic acid micelles for gene delivery: properties and in vitro transfection studies. Int J Pharm 2006;315:158–66.
[23] Ohya Y, Cai R, Nishizawa H. Preparation of PEG-grafted chitosan particle for peptide drug carrier. Proc Intl Symp Control Rel Bioact Mater 1999;26:655–6.
[24] Zhang C, Ding Y, Yu LL, Ping QN. Polymeric micelle systems of hydroxycamptothecin based on amphiphilic *N*-alkyl-*N*-trimethyl chitosan derivatives. Colloids Surf B Biointerfaces 2007;55:192–9.
[25] Zhang C, Ping QN, Zhang HG, Shen J. Preparation of *N*-alkyl-*O*-sulfate chitosan derivatives and micellar solubilization of Taxol. Carbohydr Polym 2003;54:137–41.
[26] Alexander MS, Kiser MM, Culley T, Kern JR, Dolan JW, McChesney JD, et al. Measurement of PTX in biological matrices: high-throughput liquid chromatographic-tandem mass spectrometric quantification of PTX and metabolites in human and dog plasma. J Chromatogr B Analyt Technol Biomed Life Sci 2003;785:253–61.
[27] Nishiyama N, Kataoka K. Current state, achievements, future prospects of polymeric micelles as nanocarriers for drug and gene delivery. Pharmacol Ther 2006;112:630–48.
[28] Rowinsky EK, Donehower RC. The clinical pharmacology of paclitaxel (Taxol). Semin Oncol 1993;20:16–25.
[29] Patel HM. Serum opsonin and liposomes: their interaction and opsonophagocytosis. Crit Rev Ther Drug Carrier Syst 1992;9:39–90.
[30] Ketai LH, Muggenberg BA, McIntire GL, Bacon ER, Rosenberg R, Losco PE, et al. CT imaging of intrathoracic lymph nodes in dogs with bronchoscopically administered iodinated nanoparticles. Acad Radiol 1999;6:49–54.
[31] Gianni L, Kearns CM, Capri G, Vigano L, Locatelli A, Bonadonna G, et al. Nonlinear pharmacokinetics and metabolism of paclitaxel and its pharmacokinetic/pharmacodynamic relationships in humans. J Clin Oncol 1995;13:180–90.
[32] Sparreboom A, Tellingen O, Nooijen WJ, Beijnen JH. Nonlinear pharmacokinetics of paclitaxel in mice results from the pharmaceutical vehicle Cremophor EL. Cancer Res 1996;56:2112–5.
[33] Yeh TK, Lu Z, Wientjes MG, Au JLS. Formulating paclitaxel in nanoparticles alters its disposition. Pharm Res 2005;22:867–74.